IOPscience iopscience.iop.org

Home Search Collections Journals About Contact us My IOPscience

Higher vibrational states of OH/OD in the bulk of congruent $LiNbO_3$ and in proton/deuteron exchanged layers at the surface of $LiNbO_3$

This article has been downloaded from IOPscience. Please scroll down to see the full text article.

1995 J. Phys.: Condens. Matter 7 6393

(http://iopscience.iop.org/0953-8984/7/32/006)

View the table of contents for this issue, or go to the journal homepage for more

Download details:
IP Address: 171.66.16.151
The article was downloaded on 12/05/2010 at 21:53

Please note that terms and conditions apply.

J. Phys.: Condens. Matter 7 (1995) 6393–6405. Printed in the UK

Higher vibrational states of OH/OD in the bulk of congruent $LiNbO_3$ and in proton/deuteron exchanged layers at the surface of $LiNbO_3$

A Gröne and S Kapphan
Department of Physics, University of Osnabrück, D-49069 Osnabrück, Germany

Received 21 March 1995, in final form 15 June 1995

Abstract. The fundamental vibrational transition $\tilde{\nu}_{01}$ and the higher vibrational transitions $\tilde{\nu}_{02}$, $\tilde{\nu}_{03}$ and $\tilde{\nu}_{04}$ of the OH and the OD oscillator in the bulk of congruent $LiNbO_3$ and in proton/deuteron exchanged $LiNbO_3$:PE/DE surface layers are investigated with respect to their spectroscopic properties and their temperature dependence. All observed vibrational transitions are completely polarized perpendicular with respect to the ferroelectric z direction. The spectral positions of the vibrational transitions follow closely a Morse type potential with $D_e = 4.75$ eV and $a = 22.23$ nm^{-1} ($\omega_{e,OH} = 3684$ cm^{-1} and $\omega_e x_{e,OH} = 88.5$ cm^{-1} for $LiNbO_3$:PE). No hint of possible hydrogen bonding was found. The integrated absorption intensity ratios of the higher vibrational transitions exhibit the existence of an electrical anharmonicity, i.e. a non-linearity of the dipole moment versus O–H separation. The electrical anharmonicity reveals a noticeable temperature dependence whereas the vibrational transition energies and therefore the mechanical anharmonicity shows no temperature dependence in the range from room temperature to liquid helium temperature.

1. Introduction

Hydrogen impurities, i.e. protons, being present in as-grown $LiNbO_3$, or introduced by treatment in humid or acid atmosphere, influence properties which are important for applications like the thermal fixing of volume holograms [1], the production of wave guiding layers by proton exchange [2] or implantation [3], the dark conductivity [4] and changes in the refractive index of the crystal, thereby varying the phase matching temperature for optical second harmonic generation [5].

Hydrogen centres in the bulk of the ususally congruent, non-stoichiometric, $LiNbO_3$ (at 48.4 mol% Li_2O the phase diagram shows an equal composition of the melt and the crystal [6, 29], allowing the growth of large homogeneous crystal boules) exhibit their existence by a characteristic OH stretching vibration at about 3485 cm^{-1} with a halfwidth of $\approx$30 cm^{-1}. This broad band is completely polarized perpendicular to the ferroelectric z-axis [6]. A decomposition fit reveals that the absorption band is a composition of three to four bands in the congruent material [7]. Below $T = 293$ K this broad absorption band shows almost no temperature dependence. Even in stoichiometric $LiNbO_3$ (after vapour transport equilibration, VTE), where the halfwidth of the OH absorption band becomes smaller by more than an order of magnitude, recent measurements [8] have shown only a very small shift of the band position from room temperature to LHe temperature.

High OH (OD) concentrations at the surface of $LiNbO_3$ can be fabricated by proton (deuteron) exchange [2]. The associated broad OH (OD) stretching vibrations (FWHM $\approx$30

0953-8984/95/326393+13$19.50 © 1995 IOP Publishing Ltd

(21) cm^{-1}) are again polarized perpendicular to the z-axis, and the absorption maximum shifts to 3507 (2589) cm^{-1}.

The transition energies to the higher excited vibrational states yield the mechanical anharmonicity and the integrated intensity ratios reveal the contribution of the electrical anharmonicity, i.e. the non-linearity of the dipole moment versus the O–H separation.

Despite the importance of the protons very little is known about the microscopic OH defect model parameters. Only recently could it be clarified from isotopic variations ($H^+ \leftrightarrow D^+$) that protons and deuterons, respectively, and not OH^- or OD^- ions are active in the migration process responsible for the protonic dark conductivity at elevated temperatures [4]. The isotropic activation energy for migration of the protons [4] of about 1.2 eV being much smaller than the dissociation energy of about 4.5 eV of the stretching vibration [9] and the large halfwidth (FWHM ~ 30 cm^{-1}) of the OH absorption band in congruent $LiNbO_3$ lead to speculations about possible contributions of hydrogen bonding [10]. In this case the spectral position of the absorption peak is expected to shift to much smaller wavenumbers with respect to the spectral position of the free OH radical. Furthermore the absorption band should exhibit a large halfwidth and a tunnelling splitting of the energy levels—visible in particular close to the top of the potential barrier where the remaining height and width of the potential barrier is small and the tunnelling splitting will be large.

Since the spectral positions of the higher vibrational transitions reveal the form of the potential directly, they should be suited to give decisive information about the diatomic oscillation in a double- [11] or single-well [9] potential, particularly, whenever the transition energy is close to or exceeds the energy barrier. The observation of higher vibrational transitions is a difficult task since the integrated intensity as well as the absorption coefficient of each of the next higher transitions will be smaller by about two orders of magnitude compared to the previous one. The intensity of higher vibrational transitions in hydrogen bonded systems is expected to be reduced even more drastically [12]. Therefore special preparations and high sensitivity of the spectroscopic measurements are required.

Extending earlier investigations [9] of the OH/OD vibrational transitions $\tilde{\nu}_{01}$ and $\tilde{\nu}_{02}$ we therefore looked for higher vibrational transitions $\tilde{\nu}_{03}$ and $\tilde{\nu}_{04}$ of the OH/OD oscillator in the bulk of congruent $LiNbO_3$ and in proton/deuteron exchanged $LiNbO_3$ surface layers.

2. Experimental techniques

For the investigations of the higher excited vibrational states of the OH/OD stretching mode proton/deuteron exchanged (PE/DE) $LiNbO_3$ layers have been produced by immersion of thin z-cut samples (thickness $d = 0.5$ mm) in benzoic/deuterated benzoic acid melt at 517 K for 70 hours. To avoid damage of the exchanged surface a buffering of 0.5 mol% lithium benzoate was added to the melt. The exchanged layers have a thickness up to 10 μm and an absorption coefficient of $\alpha_{max} \approx 9 \times 10^3$ cm^{-1} [13]. Due to an atmosphere which is not completely dry during the deuteron exchange process some protons are seen to enter the crystal as well. The absorption a_{OD} per OD ion is smaller than the absorption a_{OH} per OH ion ($a_{OH}/a_{OD} \approx 1.3$) [4]. For this reason the integrated optical density of the OD vibration is smaller than the integrated optical density of the OH vibration for the same thickness of the exchanged layer produced under the same proton/deuteron exchange process parameters.

Large, homogeneous crystal samples of the congruent composition (at 48.4 mol % Li_2O melt and crystal composition are the same [29]), grown using the Czochralski method, have been obtained either from Crystal Technology, USA, or the crystal growth laboratory of the University of Sao Paulo, Sao Carlos Campus, Brazil. To raise the Li content in selected samples to the stoichiometric concentration, thin crystal slices are heated in our

own laboratory [8] in a Li-rich atmosphere at $T = 1100$ °C for extended periods (vapour transport equilibration technique from $LiNbO_3/Li_3NbO_4$ phase mixtures).

Higher vibrational transitions are difficult to observe due to the small absorption coefficients. This requires special preparation. For the weak absorptions of the higher vibrational states the thin proton/deuteron exchanged $LiNbO_3$ sample has been used as an optical waveguide (see figure 1) leading to an estimated optical density $\log(I_0/I)$ of the fundamental OH stretching vibration of about ~700. So the weak higher vibrational transitions of the OH/OD oscillator in proton/deuteron exchanged $LiNbO_3$:PE/DE could be detected. Direct end coupling of the measurement light into the proton/deuteron exchanged waveguide layer of the crystal was not possible due to the geometry of the sample chamber and the focusing of the divergent light beam in the Fourier IR spectrometer.

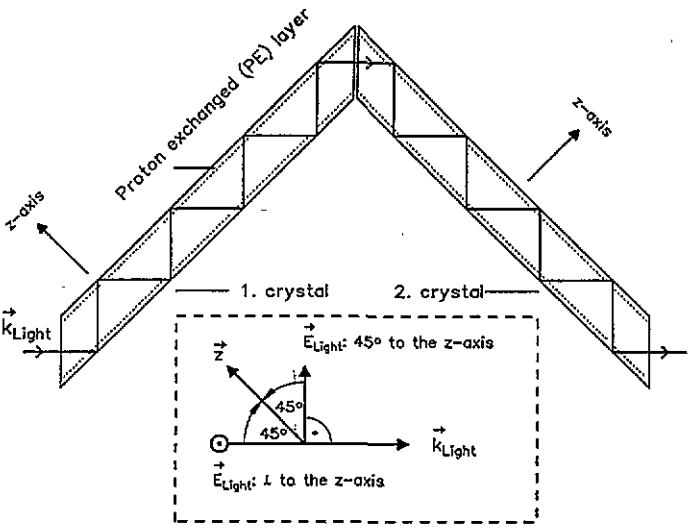

Figure 1. Experimental set-up for the investigations of the higher vibrational transitions of the OH (OD) oscillator in proton (deuteron) exchanged $LiNbO_3$:PE (DE). Due to the total reflexion the wave vector k_{Light} of the light always inclines at an angle of 45° with respect to z. The crystals have a thickness of 0.5 mm and a length of 20 mm. For this set-up the effective optical path through the exchanged layers amounts to about 2.2 mm.

The hydrogen concentration in the bulk of congruent $LiNbO_3$ was raised in poled, single-crystalline samples of perfect optical quality by field supported proton diffusion [9]. An electric DC field of 100 V cm^{-1} was applied perpendicular to the z-axis at $T = 650$ °C for about 20 min, raising the OH absorption coefficient $\alpha_{max,OH}$ to about 15 cm^{-1}.

The infrared absorption spectra were obtained with a Fourier IR spectrometer 113 Cv (Bruker) in the range from 2000 cm^{-1} to 15000 cm^{-1} with a maximal resolution of about 0.05 cm^{-1}. For the measurements of the temperature dependence of the absorption bands from 293 K to 1.5 K we used a Leybold helium cryostat.

3. Results and discussion

3.1. Spectroscopic positions of higher vibrational transitions

The absorption spectra of the OH/OD fundamental stretching vibration and its first overtone in the bulk of congruent $LiNbO_3$ and in proton/deuteron exchanged $LiNbO_3$:PE (DE), always

polarized completely perpendicular to z, have been reported earlier [9].

The weak absorption band of the second overtone ($\tilde{\nu}_{03}$) of the OH stretching vibration in the bulk of congruent $LiNbO_3$ is shown in figure 2. Despite their small intensities the new absorption spectra of the second overtone $\tilde{\nu}_{03,PE}/\tilde{\nu}_{03,DE}$ and the third overtone $\tilde{\nu}_{04,PE}/\tilde{\nu}_{04,PE}$ of the OH/OD vibration in $LiNbO_3$:PE/DE could be unambiguously detected and are shown in figures 3 and 4.

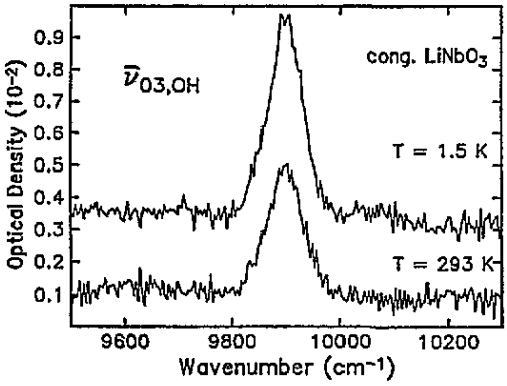

Figure 2. Second overtone ($\tilde{\nu}_{03}$) of the OH stretching vibration in the bulk of congruent $LiNbO_3$ at RT (bottom) and LHeT (top). The crystal thickness is $d = 1.65$ cm and the optical density $OD_{max} = 0.004$ at RT. This yields an absorption coefficient $\alpha_{max,03} = 0.0055$ cm^{-1}. The spectra are recorded with linear polarized light: $E_{Light} \perp z \perp k_{Light}$. The spectra are shifted vertically for better viewing.

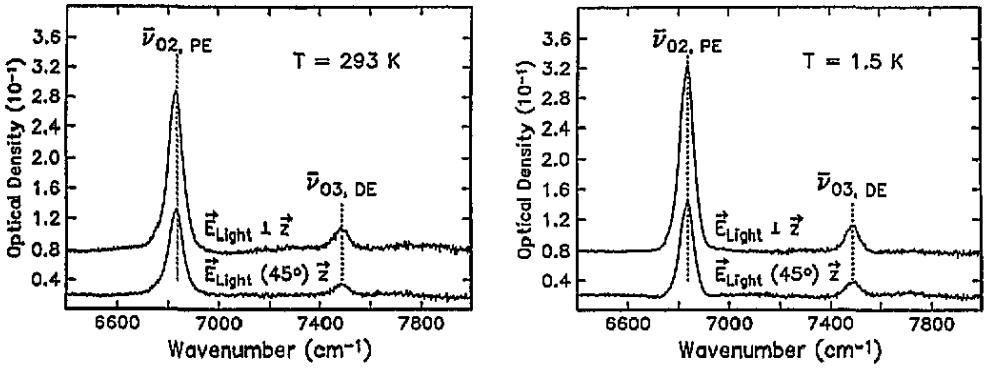

Figure 3. Higher OH and OD vibrational transitions ($\tilde{\nu}_{02,PE} = 6836$ cm^{-1} and $\tilde{\nu}_{03,DE} = 7487$ cm^{-1}) in deuteron exchanged $LiNbO_3$:DE at RT (left) and LHeT (right). The wave vector k_{Light} of the light inclines an angle of 45° with respect to z. The polarization of the light E_{Light} is perpendicular ($\perp$) with respect to z (top) and inclines an angle of 45° with respect to z (bottom). The vibrational transitions $\tilde{\nu}_{02,PE}$ and $\tilde{\nu}_{03,PE}$ for this experimental set-up exhibit the expected ratio for the incidence of linear polarized light: $I_{45°}/I_{\perp} = 0.5$. The spectra are shifted vertically for better viewing.

The absorption bands of the higher vibrational transitions of the OH/OD oscillator in the bulk of congruent $LiNbO_3$ as well as in proton/deuteron exchanged $LiNbO_3$:PE/DE exhibit a linear dependence on the OH/OD concentration and show the expected polarization dependence of the transitions polarized completely perpendicular to the polar z direction of $LiNbO_3$.

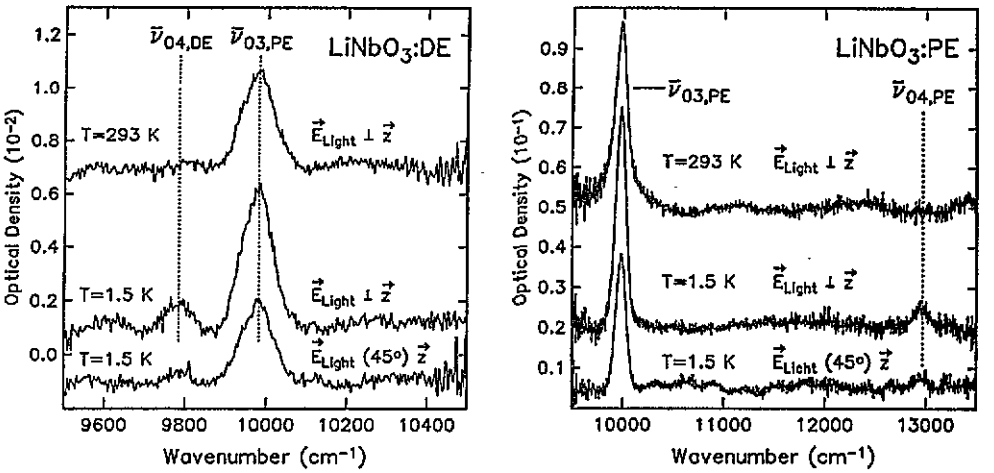

Figure 4. Higher OH and OD vibrational transitions $\bar{\nu}_{03,PE} = 9989\ cm^{-1}$, $\bar{\nu}_{04,PE} = 12\,965\ cm^{-1}$ and $\bar{\nu}_{04,DE} = 9783\ cm^{-1}$ in deuteron exchanged $LiNbO_3$:DE (left) and in proton exchanged $LiNbO_3$:PE (right) at RT (top) and LHeT (middle and bottom). The wave vector k_{Light} of the light inclines an angle of 45° with respect to z. The polarization of the light E_{Light} is perpendicular (⊥) with respect to z (top and middle) and inclines an angle of 45° with respect to z (bottom). The vibrational transitions $\bar{\nu}_{03,PE}$, $\bar{\nu}_{04,PE}$ and $\bar{\nu}_{04,DE}$ exhibit in this experimental set-up the ratio expected for the incidence of linear polarized light: $I_{45°}/I_{\perp} = 0.5$. The spectra are shifted vertically for better viewing.

The absorption per OH ion and therefore the oscillator strength of OH in the bulk and in proton exchanged layers of $LiNbO_3$ has been shown experimentally to be the same both for congruent [14] and for stoichiometric (VTE) $LiNbO_3$ [8].

Even for the larger halfwidths of the vibrational OH transitions in proton exchanged $LiNbO_3$ systems, the evaluation of the vibrational transition wavenumbers $\bar{\nu}_{01}$, $\bar{\nu}_{02}$, $\bar{\nu}_{03}$ and $\bar{\nu}_{04}$ gives information about the form of the average oscillator potential. The vibrational energy levels $G_n = E_n/(hc)$ and consequently the transition wavenumbers $\bar{\nu}_{0n} = G_n - G_0$ of an average anharmonic diatomic oscillator described by a Morse potential $V(r) = D_e(1 - e^{-a(r-r_e)})^2$ are given by [15]

$$G_n = \omega_e(n + 1/2) - \omega_e x_e(n + 1/2)^2 \tag{1}$$

with

$$\omega_e x_e = \frac{a^2\hbar}{2\mu_m} \qquad \omega_e = a\sqrt{\frac{2D_e}{\mu_m}}. \tag{2}$$

μ_m is the reduced mass, r_e the O–H nuclear equilibrium separation, D_e the potential depth and $h = \hbar 2\pi$ Planck's constant.

3.1.1. Higher vibrational transitions of OH in the bulk of congruent $LiNbO_3$ at room temperature. For the OH oscillator in the bulk of congruent $LiNbO_3$ we derive from the spectral position of the fundamental ($\bar{\nu}_{01} = 3484(\pm 2)\ cm^{-1}$) and its first overtone ($\bar{\nu}_{02} = 6783(\pm 4)\ cm^{-1}$) the spectroscopic parameters $\omega_{e,OH} = 3670\ cm^{-1}$ and $\omega_e x_{e,OH} = 93\ cm^{-1}$. Assuming a Morse type potential the spectral position of the second overtone ($\bar{\nu}_{03}$) of the OH stretching vibration can be calculated according to equation (1). The calculated wavenumber $\bar{\nu}_{03,calc} = 9894\ cm^{-1}$ agrees perfectly with the observed wavenumber $\bar{\nu}_{03} =$

9894 (± 8) cm^{-1}. This indicates that the description of the average diatomic OH centre by a Morse type potential is justified.

By isotopic exchange one can check wether the description of the OH oscillator and the OD oscillator by the same Morse potential is justified. With $\rho = \mu_{m,OH}/\mu_{m,OD}$ as the ratio of the reduced masses the transition energies after isotopical exchange are:

$$G_{n,OD} = \sqrt{\rho}\omega_{e,OH}\ (n + 1/2) - \rho\omega_e x_{e,OH}\ (n + 1/2)^2. \tag{3}$$

If we use in a first approximation the reduced mass of the free anharmonic oscillator $\mu_{m,free,OH} = m_H m_O/m_H + m_O = 0.9412$ a.m.u., which assumes no coupling of the vibrating molecule to the lattice, with the spectroscopic parameters $\omega_{e,OH}$ and $\omega_e x_{e,OH}$ of the OH oscillator the spectroscopic parameters (see table 1) and the vibrational transition wavenumbers of the OD oscillator are calculated: $\bar{\nu}_{01,OD,calc} = 2572(\pm 3)$ cm^{-1} and $\bar{\nu}_{02,OD,calc} = 5045(\pm 3)$ cm^{-1}, which do not yet perfectly agree with the observed OD wavenumbers $\bar{\nu}_{01,OD,obs} = 2574(\pm 2)$ cm^{-1} and $\bar{\nu}_{02,OD,obs} = 5054(\pm 4)$ cm^{-1}. Fowler *et al* [16] have introduced a simple model where the OH/OD oscillator is coupled through the oxygen atom to the lattice. The reduced mass can be described by the expression $\mu_{m,coup,OH} = m_H(1 - m_H/m_O) = 0.9375$ a.m.u. Then the computed OD wavenumbers amount to $\bar{\nu}_{01,OD,calc} = 2586(\pm 3)$ cm^{-1} and $\bar{\nu}_{02,OD,calc} = 5073(\pm 3)$ cm^{-1}. There is still a small discrepancy with the observed OD wavenumbers. On the other hand the real ratio of the reduced masses $\rho = \mu_{m,OH}/\mu_{m,OD}$ of the OH/OD oscillator in the crystal can be determined from the ratio of the OH and OD fundamental absorptions according to equations (1) and (3)

$$\frac{\bar{\nu}_{01,OD}}{\bar{\nu}_{01,OH}} = \frac{\Delta G_{01,OD}}{\Delta G_{01,OH}} = \frac{\sqrt{\rho} - 2\rho x_{e,OH}}{1 - 2x_{e,OH}}. \tag{4}$$

Evaluating the last equation yields $\rho = 0.5304$ and inserting this value in equation (3) the first overtone of the OD oscillator can be calculated as $\bar{\nu}_{02,OD,calc} = 5050(\pm 4)$ cm^{-1} which is within experimental error equal to the observed value. This shows that the OH and OD oscillators in the bulk of congruent $LiNbO_3$ can be described very well by the same Morse potential.

Table 1. Calculated Morse potential parameter for the OH and OD oscillator in $LiNbO_3$ using the reduced mass of the free diatomic oscillator $\mu_{m,free}$. The mechanical anharmonicity parameters $\omega_e x_{e,OH}$ and $\omega_{e,OH}$ are calculated according to equation (1). According equation (2) D_e and a are determined. With these values the parameters for the OD oscillator $\omega_{e,OD}$ and $\omega_e x_{e,OD}$ are calculated according to equation (2).

	Congruent		PE / DE	
	OH	OD	OH	OD
	$\mu_{m,free}$	$\mu_{m,free}$	$\mu_{m,free}$	$\mu_{m,free}$
ω_e (cm^{-1})	3670±10	2670±8	3684±10	2681±8
$\omega_e x_e$ (cm^{-1})	93 ± 4	49 ± 3	89 ± 4	47 ±3
D_e (eV)	4.5± 0.2		4.7 ± 0.2	
a (nm^{-1})	22.8 ± 0.4		22.2 ± 0.4	

3.1.2. Higher vibrational transitions of OH/OD in $LiNbO_3$:PE/DE at room temperature
Assuming a Morse type potential the spectral position of the third OH overtone $\bar{\nu}_{04}$ should

exceed the activation energy $E_A \approx 1.2$ eV of the protonic conductivity and amount to a value of $\bar{\nu}_{04} \approx 1.6$ eV.

To get information about the spectral position of the third overtone we extend the investigations of the higher vibrational transitions on proton/deuteron exchanged $LiNbO_3$:PE/DE. In these proton/deuteron exchanged surface layers very high optical densities of the OH/OD stretching vibration can be reached, especially by using the set-up mentioned above.

For the OH oscillator in proton exchanged $LiNbO_3$:PE we determined the mechanical anharmonicity to be $\omega_e x_{e,OH} = 88.5\,cm^{-1}$ and $\omega_{e,OH} = 3684\ cm^{-1}$. With these values the vibrational transition energies $\bar{\nu}_{03}$ and $\bar{\nu}_{04}$ of the higher excited states are calculated and compared with the experimental observed energies (see table 2).

Table 2. Observed vibrational transition energies $\bar{\nu}_{0n,PE/DE}$ and values calculated on the basis of a Morse type potential for the OH/OD vibration in proton/deuteron exchanged (PE/DE) $LiNbO_3$. The potential parameters for the calculations of the wavenumbers $\bar{\nu}_{0n}$ are $D_e = 4.75$ eV and $a = 22.23\ nm^{-1}$ (see table 1). The last row shows the observed halfwidths $\delta\bar{\nu}$ (FWHM).

$LiNbO_3$:PE	$\bar{\nu}_{01,PE}$ (cm^{-1})	$\bar{\nu}_{02,PE}$ (cm^{-1})	$\bar{\nu}_{03,PE}$ (cm^{-1})	$\bar{\nu}_{04,PE}$ (cm^{-1})
Observed	3508 ± 2	6836 ± 4	9989 ± 8	12965 ± 16
Calculated	*3507 ± 2*	*6837 ± 4*	*9990 ± 18*	*12966 ± 40*
$\delta\bar{\nu}$ (FWHM)	30 ± 2	67 ± 3	127 ± 6	170 ± 10
$LiNbO_3$:DE	$\bar{\nu}_{01,DE}$(cm^{-1})	$\bar{\nu}_{02,DE}$ (cm^{-1})	$\bar{\nu}_{03,DE}$ (cm^{-1})	$\bar{\nu}_{04,DE}$(cm^{-1})
Observed	2588 ± 2	5084 ± 4	7487 ± 8	9783 ± 12
Calculated	2587 ± 2	5081 ± 3	7481 ± 12	9788 ± 28
$\delta\bar{\nu}$ (FWHM)	21 ± 2	46 ± 3	65 ± 5	85 ± 8

Using the reduced mass of the free diatomic oscillator the spectroscopic parameters for the OD vibration are also determined (see table 1). With these values the fundamental and the higher vibrational transition energies of the OD oscillator are calculated and compared with the observed OD transition wavenumbers $\bar{\nu}_{0n,DE}$ (see table 2).

The calculated and observed transition energies $\bar{\nu}_{01,PE}$ up to $\bar{\nu}_{04,PE}$ as well as $\bar{\nu}_{01,DE}$ up to $\bar{\nu}_{04,DE}$ fit so closely, confirming the above diatomic Morse potential, that very little room remains for other possibilities. In particular, a double-well potential (for example see figure 5) would lead to a shift and possible (tunnelling) splitting of the vibrational levels, which is not observed. A tunnelling reorientation of the OH ions at low temperature under applied electric field or uniaxial stress could not be observed either in $LiNbO_3$ or in any of the ABO_3 perovskite lattices [17]. Even in the stoichiometric (VTE) $LiNbO_3$ where the halfwidth of the OH vibrational transition is smaller by about one order of magnitude and for the first time a temperature dependence of the vibrational OH transitions $\bar{\nu}_{01}$ and $\bar{\nu}_{02}$ could be observed, no line splitting or structure due to possible tunnelling splitting could be detected [8].

Moreover the transition energy of the fourth excited vibrational state $\bar{\nu}_{04,PE} = 1.608$ eV of the OH oscillator in proton exchanged $LiNbO_3$:PE is much higher than the activation energy $E_A \approx 1.2$ eV of the protonic conductivity [4] and is also higher than the energy barrier (height about 1.2 eV) separating the double wells in our example in figure 5. This excludes the assumption that the OH molecules vibrate along the oxygen–oxygen bonding with thermally activated hopping from one potential well along the O–O bonding to a

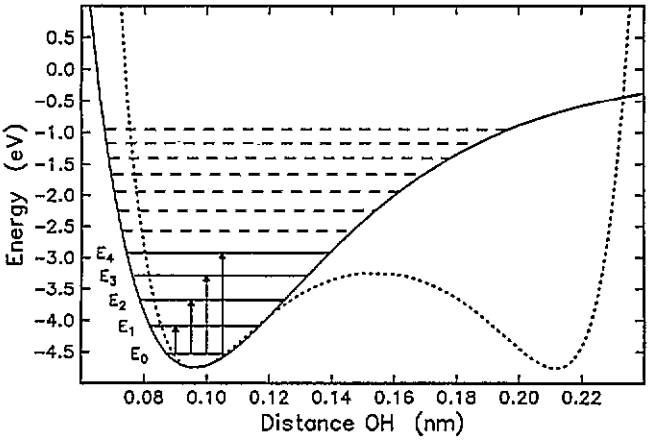

Figure 5. Morse potential $V(r) = D_e\left(e^{-2a(r-r_e)} - 2e^{-a(r-r_e)}\right)$ with $D_e = 4.75$ eV, $a = 22.31$ nm^{-1} and $r_e = 0.096$ nm (full line) and calculated vibrational energy levels (horizontal lines). The vertical arrows mark the observed vibrational transitions of the OH oscillator in proton exchanged $LiNbO_3$:PE. Dotted line: example for a double-minimum Morse potential with an energy barrier of $E_b \approx 1.2$ eV ($V(r) = D(2e^{-2a(R-r_0)}\cosh(2ar) - 4e^{-a(R-r_0)}\cosh(ar)) - D$, $r_0 = 0.096$ nm, $R = 0.154$ nm, $a = 40$ nm^{-1}, $D = 2.36$ eV) [11].

neighbouring potential well separated by a barrier of the size of the activation energy E_A. For the discussion of the activation energy of the protonic mobility in TiO_2 a librational motion as an attempt frequency has been introduced for the OH oscillator [18]. A random-walk model for thermally activated diffusion in one direction gives $D_0 = \frac{1}{2}\nu_a d^2$ for the pre-exponential factor D_0 of the Arrhenius expression $D = D_0 \exp(E_A/(kT))$ where d signifies the jump distance and ν_a the attempt frequency. The calculations for TiO_2 involving the librational mode as an attempt frequency can explain the discrepancy between the potential depth D_e of the stretching vibration and the activation energy E_A of the protonic conductivity. Moreover in $LiNbO_3$ the protonic conductivity is isotropic whereas the stretching vibration is completely polarized perpendicular to z. For all these reasons the frequency of the vibrational mode cannot be the attempt frequency for the protonic hopping conductivity in $LiNbO_3$. However, we have found for the first time a direct OH and OD libration in $LiNbO_3$ (with isotropic librational properties) which can serve as an attempt frequency similiar to the description above [18]. Also a libration+vibration combination band has been found for the first time. The results will be presented elsewhere [19].

3.2. Integrated intensities of higher vibrational transitions

The linear dipole moment approximation, $\mu(r) = M_0 + M_1(r - r_e)$, predicts an integrated intensity ratio $I_{0n}/I_{01} \approx (n-1)!\,x_e^{n-1}$, using Morse oscillator eigenfunctions [20]. For proton exchanged $LiNbO_3$ the experimentally observed intensity ratio $I_{01}/I_{02} = 165$ is in strong contradiction to the expected ratio of $I_{01}/I_{02} \approx x_e^{-1} = 39$ assuming a linear dipole moment. Therefore one has to take electrical anharmonicity, i.e. the non-linearity of the dipole moment versus O–H separation, into account to match the observed intensity ratio I_{01}/I_{02}. Now one also has to consider the higher derivatives of the dipole moment [21].

The absorption I_{0n} from the ground state $|\psi_0\rangle$ to the n-excited vibrational state $|\psi_n\rangle$ is

given by [22]

$$I_{0n} \sim N_0 \bar{\nu}_{0n} |R_{0n}|^2 \qquad R_{0n} = \int_0^\infty \psi_0(r)\, \mu(r)\, \psi_n(r)\, \mathrm{d}r. \tag{5}$$

$\bar{\nu}_{0n}$ = transition wavenumber, N_0 = population of the ground state, R_{0n} = the matrix element of the dipole moment for the transition $|\psi_0\rangle \rightarrow |\psi_n\rangle$ and ψ_n = eigenfunction of the nth vibrational level.

The dipole moment $\mu(r)$ may be developed into a polynomial about the equilibrium nuclear separation r_e:

$$\mu(r) = M_0 + M_1 (r - r_e) + M_2 (r - r_e)^2 + M_3 (r - r_e)^3 + M_4 (r - r_e)^4 + \ldots. \tag{6}$$

We define

$$S_{\mathrm{I}}^{0n} \equiv \int_0^\infty \psi_0(r)\, (r - r_e)\, \psi_n(r)\, \mathrm{d}r \qquad S_{\mathrm{II}}^{0n} \equiv \int_0^\infty \psi_0(r)\, (r - r_e)^2\, \psi_n(r)\, \mathrm{d}r$$

$$S_{\mathrm{III}}^{0n} \equiv \int_0^\infty \psi_0(r)\, (r - r_e)^3\, \psi_n(r)\, \mathrm{d}r \qquad S_{\mathrm{IV}}^{0n} \equiv \int_0^\infty \psi_0(r)\, (r - r_e)^4\, \psi_n(r)\, \mathrm{d}r. \tag{7}$$

Neglecting terms higher than fourth order in $\mu(r)$ and introducing (6) into (5) by using (7) leads to

$$\frac{I_{0l}}{I_{0n}} \frac{\bar{\nu}_{0n}}{\bar{\nu}_{0l}} = \left| \frac{R_{0l}}{R_{0n}} \right|^2 = \left(\frac{S_{\mathrm{I}}^{0l} + \frac{M_2}{M_1} S_{\mathrm{II}}^{0l} + \frac{M_3}{M_1} S_{\mathrm{III}}^{0l} + \frac{M_4}{M_1} S_{\mathrm{IV}}^{0l}}{S_{\mathrm{I}}^{0n} + \frac{M_2}{M_1} S_{\mathrm{II}}^{0n} + \frac{M_3}{M_1} S_{\mathrm{III}}^{0n} + \frac{M_4}{M_1} S_{\mathrm{IV}}^{0n}} \right)^2. \tag{8}$$

By this, the ratio of the dipole moment coefficients M_2/M_1, M_3/M_1 and M_4/M_1 can be determined evaluating the ratio of the integrated absorptions, i.e. the ratio of the integrated optical densities, I_{01}/I_{02}, I_{01}/I_{03} and I_{01}/I_{04}. (Note: M_0 stays undetermined.) The intensity of the absorption I_{0n} is proportional to the square of the transition matrix element R_{0n} and therefore the evaluation of these measurements leaves a sign ambiguity for the determination of R_{0n}. Consequently several solutions exist for the ratios of the dipole moment coeffficients M_n/M_1 which fit the observed intensity ratios. To get information about the form of the dipole moment one has to bear in mind that M_n/M_1 and $(-M_n)/(-M_1)$ fit the same intensity ratios.

For the calculation of the dipole moment parameters and the transition matrix elements we use the eigenfunctions of a Morse oscillator calculated with the experimentally determined potential parameters listed in section 3.1. For r_e we choose 0.096 nm to match theoretically [23, 24] and experimentally [25, 26, 27] determined values for $\langle\psi_0|r|\psi_0\rangle \approx 0.097$ nm.

Looking at table 3 it is obvious that neither a linear dipole moment nor a quadratic or cubic dipole moment function is sufficent to describe all of the observed intensity ratios I_{0n}/I_{01} of the OH/OD oscillator in proton/deuteron exchanged $LiNbO_3$:PE/DE.

To describe the dipole moment function of a diatomic oscillator it would be helpful to have a simple explicit expression. Such an explicit dipole moment of the form $\mu(r) = kre^{-r/r^*}$ has been suggested by Sage [28] and can be used to calculate with Morse oscillator eigenfunctions the transition matrix elements analytically. The constants k and r^* are chosen to fit the computed dipole moment and are designed to allow for covalency of the OH bond [28]. The intensity ratios I_{0n}/I_{01} can be calculated as a function of the parameter r^*. The results for the intensity ratios of the OH oscillator in $LiNbO_3$:PE are shown in figure 6. As before, due to the dependence of the intensity on the square of the transition matrix element, there is not just one unambiguous parameter r^* which is able to fit all the observed intensity ratios I_{01}/I_{02}, I_{01}/I_{03} and I_{01}/I_{04}. The results for OD in

Table 3. At LHeT observed values (1 column, exp.) and intensity ratios of the OH and OD absorption bands in proton and in deuteron exchanged $LiNbO_3$:PE/DE calculated using a polynomial approximation for the dipole moment function. The intensity ratios I_{01}/I_{02}, I_{01}/I_{03} and I_{01}/I_{04} can only be fitted for $M_4/M_1 r_e^3 \neq 0$.

	Exp.	Intensity ratios calculated with dipole moment functions				
		Linear	Quadratic		Cubic	$O((r-r_e)^4)$
		$\frac{I_{01}}{I_{0n}} \approx \frac{x_e^{1-n}}{(n-1)!}$	$\frac{M_2}{M_1} r_e =$ 0.570	$\frac{M_2}{M_1} r_e =$ 0.939	$\frac{M_2}{M_1} r_e = 0.510$ $\frac{M_3}{M_1} r_e^2 = 0.520$	$\frac{M_2}{M_1} r_e = 0.511$ $\frac{M_3}{M_1} r_e^2 = 0.529$
			$\frac{M_3}{M_1} r_e^2 = 0 = \frac{M_4}{M_1} r_e^3$		$\frac{M_4}{M_1} r_e^3 = 0$	$\frac{M_4}{M_1} r_e^3 = -0.045$
$\frac{I_{01}}{I_{02}}$ (OH)	165	42	166	1170	166	166
$\frac{I_{02}}{I_{03}}$ (OH)	16	21	78	16	16	16
$\frac{I_{03}}{I_{04}}$ (OH)	8	14	95	3	84	8
$\frac{I_{01}}{I_{02}}$ (OD)	175	57	236	1970	223	228
$\frac{I_{02}}{I_{03}}$ (OD)	22	29	118	14	21	21
$\frac{I_{03}}{I_{04}}$ (OD)	15	19	192	4	12	11

Table 4. Changes of the integrated optical density I_{0n} in the range from RT to LHeT in proton exchanged $LiNbO_3$:PE, in deuteron exchanged $LiNbO_3$:DE and in the bulk of congruent $LiNbO_3$:cong. (see figure 7). The errors for the evaluation of the temperature dependence of the integrated optical densities I_{0n} can be estimated according to the observed deviations in figure 7: ± 1% for I_{01}, ± 2% for I_{02} and ± 4% for I_{03}.

	$LiNbO_3$		
	PE	DE	Cong.: OH
$\frac{I_{01}\ (\text{LHeT})}{I_{01}\ (\text{RT})}$	1.07	1.07	1.06
$\frac{I_{02}\ (\text{LHeT})}{I_{02}\ (\text{RT})}$	1.13	1.13	1.13
$\frac{I_{03}\ (\text{LHeT})}{I_{03}\ (\text{RT})}$	1.24	1.26	1.43

$LiNbO_3$:DE are analogous. A need for further discussions and theoretical considerations with respect to the dipole moment function of OH/OD centres has also been mentioned in recent literature related to this problem [16].

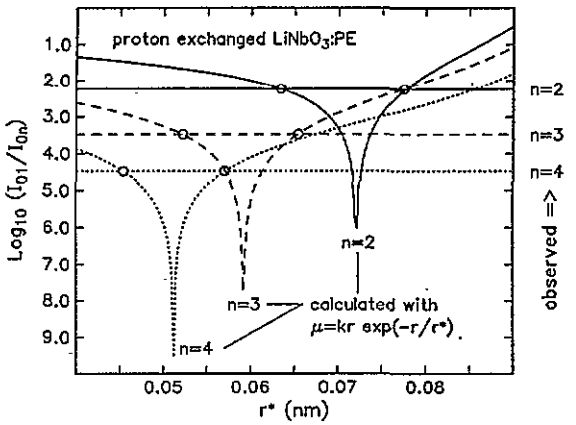

Figure 6. At LHeT observed ratios of the integrated intensities of the OH vibrational transitions I_{01}/I_{0n} (horizontal lines). Furthermore the calculated intensity ratios I_{01}/I_{0n} for OH in proton exchanged $LiNbO_3$:PE using a dipole moment $\mu(r) = kre^{-r/r^*}$ are sketched as a function of the dipole moment parameter r^*. The circles (o) mark the parameter r^* which describes the respective intensity ratio. The results for OD in deuteron exchanged $LiNbO_3$ are similiar.

3.3. Temperature dependence of higher vibrational transitions

The vibrational transition frequencies and consequently the potential of the OH and OD oscillator in the bulk of congruent $LiNbO_3$ as well as in $LiNbO_3$:PE/DE show no temperature variation in the range from 300 K to 1.5 K. Also the halfwidths show no temperature dependence. This supports the exclusion of possible hydrogen bridge bonding because with decreasing temperature and contraction of the lattice parameters a decreasing of the vibrational energy and an increasing of the halfwidth would be expected.

The temperature dependence of the electrical anharmonicity is revealed by the temperature dependence of the integrated intensity ratios of the vibrational transitions.

The OH/OD absorption coefficient in the maximum is increasing with decreasing temperature. The halfwidth and the band shape of the absorption lines reveal no temperature dependence in the range from RT to LHeT. The ratios of the integrated absorption intensities $I_{0n}/I_{01} \approx \alpha_{0n}\delta\bar{\nu}_{0n}/\alpha_{01}\delta\bar{\nu}_{01}$ and therefore the electrical anharmonicity exhibit a noticable temperature dependence (see figure 7 and table 4). The change of the integrated absorption intensity with temperature is larger for the higher vibrationally excited states. This indicates that a temperature change has an influence on the dipole moment function and therefore on the intensity ratios whereas the vibrational transition energies remain unchanged. The dipole moment function therefore displays a much stronger sensitivity to the lattice parameters with respect to slight changes of the electronic structure of the environment of the OH dipole compared with the parameters determing the form of the potential.

4. Conclusions

The transition energies of the OH (OD) absorption bands, both in the bulk and in proton/deuteron exchanged surface layers in $LiNbO_3$, can be perfectly described by a Morse potential of a diatomic anharmonic oscillator up to the OH vibrational transition $E_{04,PE} \approx$ 1.6 eV (OD: $E_{04,DE} \approx 1.2$ eV). All observed vibrational OH/OD transitions are completely polarized perpendicular to z. No indication (frequency shift or tunnelling splitting caused

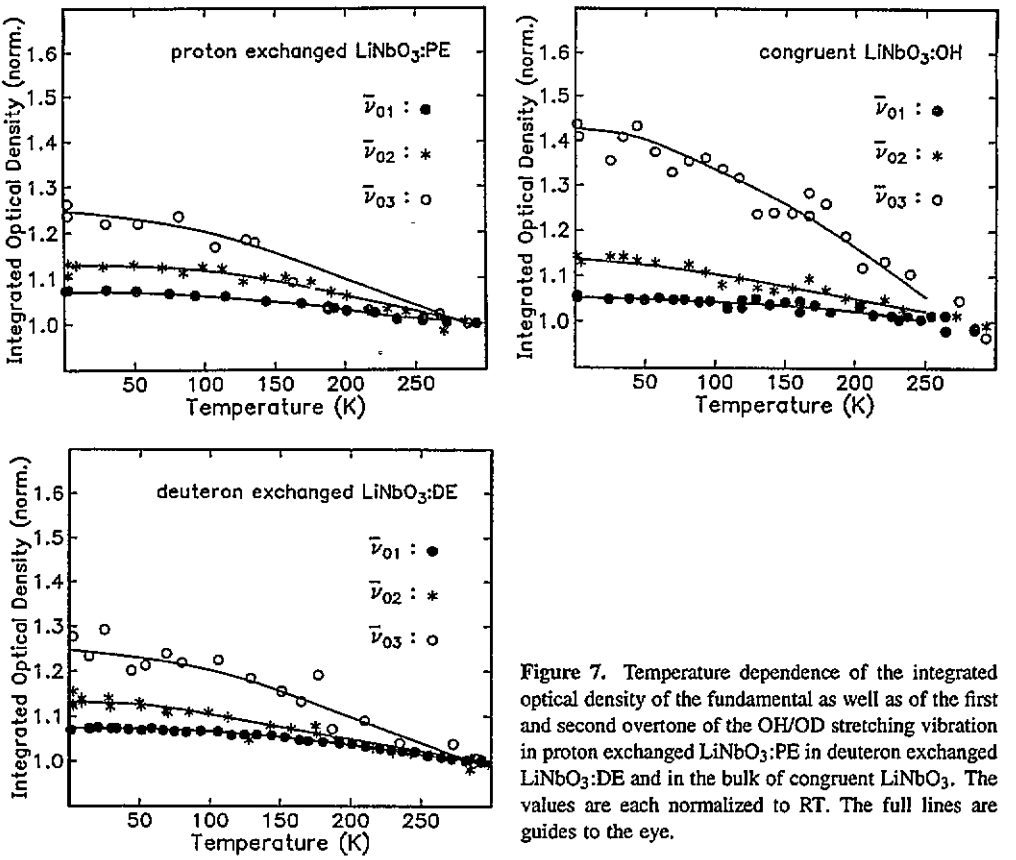

Figure 7. Temperature dependence of the integrated optical density of the fundamental as well as of the first and second overtone of the OH/OD stretching vibration in proton exchanged $LiNbO_3$:PE in deuteron exchanged $LiNbO_3$:DE and in the bulk of congruent $LiNbO_3$. The values are each normalized to RT. The full lines are guides to the eye.

by a double-well potential) for hydrogen bridge bonding is observed. Also the position of the OH stretching vibration (near 3500 cm^{-1}) and the small halfwidth (a few cm^{-1} in stoichiometric $LiNbO_3$ at room temperature [8]) together with the OH distance of about 0.1 nm from the Morse potential fit and the relation between OH stretching frequency and the R(O–O) distance [12] (the shortest O–O distance in the $LiNbO_3$ structure is 0.27 nm) all point to a very weak, if any, O–H···O hydrogen bond. The observation of the higher vibrational transitions up to $E_{04} \approx 1.6$ eV, following a simple Morse type potential for the mean value of the average OH oscillator, further excludes the assumption of any hydrogen bridge bonding. Thus the protons can no longer be assumed to hop along the O–O bonding over a potential barrier similar to figure 5 which should correspond to the activation energy $E_A = 1.2$ eV of the protonic conductivity with the frequency of the OH stretching vibration being the attempt frequency. Instead a librational motion of the OH oscillator has to be considered. Also at low temperature no tunnelling reorientation of OH ions under applied electric field or uniaxial stress could be observed.

The temperature independent mechanical anharmonicity indicates a temperature independent average Morse potential. The temperature variation of the electrical anharmonicity for OH in the bulk of congruent $LiNbO_3$ and for OH/OD in proton/deuteron exchanged $LiNbO_3$ reveals a noticable temperature dependent non-linearity of the OH/OD dipole moment function. This shows that the dipole moment is considerably influenced by slight changes of the electronic structure with temperature whereas the average potential is not affected.

The ratios of the integrated absorption intensities indicate that neither a polynomial of third order nor a dipole moment of the form [16] $\mu(r) = kre^{-\frac{r}{r^*}}$ match completely all observed intensity ratios I_{02}/I_{01}, I_{03}/I_{01} and I_{04}/I_{01}. Therefore further theoretical considerations will be necessary for a complete description.

Acknowledgments

The authors are grateful to Professor J P Andreeta USP, Sao Paulo, Brazil for supplying some of the $LiNbO_3$ crystals used. This work was supported by the Deutsche Forschungsgemeinschaft (SFB225/C7).

References

[1] Vormann H, Weber G, Kapphan S and Krätzig E 1981 *Solid State Commun.* **40** 543
[2] Jackel J L, Rice C E and Veselka J J 1982 *Appl. Phys. Lett.* **41** 607
[3] Moretti P, Thevenard P, Wirl K, Hertel P, Hesse H, Krätzig E and Godefroy G 1992 *Ferroelectrics* **128** 13
[4] Klauer S, Wöhlecke M and Kapphan S 1992 *Phys. Rev.* B **45** 2786
[5] Schmidt N, Betzler K, Grabs M, Kapphan S and Klose F 1989 *J. Appl. Phys.* **65** 1253
[6] Herrington J H, Dischler B, Räuber A and Schneider J 1973 *Solid State Commun.* **12** 351
[7] Kovác L, Wöhlecke M, Jovanović A, Polgár K and Kapphan S 1991 *J. Phys. Chem. Solids* **52** 797
[8] Gröne A and Kapphan S 1995 *J. Phys. Chem. Solids* **56** 687
[9] Förster A, Kapphan S and Wöhlecke M 1987 *Phys. Status Solidi* b **143** 755
[10] Loni A, De La Rue R M and Winfield J M 1987 *J. Appl. Phys.* **61** 64
[11] Lawrence M C and Robertson G N 1980 *Ferroelectrics* **25** 363
[12] Novak A 1974 *Struct. Bonding* **18** 177
[13] Kapphan S and Breitkopf A 1992 *Phys. Status Solidi* a **133** 159
[14] Richter R, Bremer T, Hertel P and Krätzig E 1989 *Phys. Status Solidi* a **114** 765
[15] Morse P M 1992 *Phys. Rev.* **34** 57
[16] Fowler W B, Capelletti R and Colombi E 1991 *Phys. Rev.* B **44** 2961
[17] Weber G, Kapphan S and Wöhlecke M 1986 *Phys. Rev.* B **34** 8406
[18] Bates J B, Wang J C and Perkins R A 1979 *Phys. Rev.* B **19** 4130
[19] Gröne A and Kapphan S 1995 *Radiat. Eff. Defects Solids* **132** to be published
[20] Rosenthal J E 1935 *Proc. Natl. Acad., Wash.* **21** 281
[21] Heaps H S and Herzberg G 1952 Z. *Phys.* **133** 48
[22] Schutte C 1976 *The Theory of Molecular Spectroscopy, Vol. I (The Quantum Mechanics and Group Theory of Vibrating and Rotating Molecules)* (Amsterdam: North Holland; New York: Elsevier)
[23] Werner H J, Rosmus P and Reinsch E A 1983 *J. Chem. Phys.* **79** 905
[24] Langhoff S R, Bauschlicher C W and Taylor P R 1989 *J. Chem. Phys.* **91** 5953
[25] Huber K P and Herzberg G 1979 *Molecular Spectra and Molecular Structure Constants of Diatomic Molecules* (New York: Van Nostrand)
[26] Branscomb L M 1966 *Phys. Rev.* **148** 11
[27] Owrutsky J C, Rosenbaum N H, Tack L M and Saykally R J 1985 *J. Chem. Phys.* **83** 5338
[28] Sage M L 1978 *Chem. Phys.* **35** 375
[29] Svaasand L O, Eriksrud M, Nakken G and Grande A P 1974 *J. Cryst. Growth* **22** 230